Balanced ionic conductivity and permselectivity of cation exchange membranes prepared from sulfonated poly(ether sulfone)

*Hussien K. Srour [a], Mizuki Inoue [a], Edhuan Ismail [a], Minato Higa [b], Mitsuru Higa [b], László Szabó [c], and Izumi Ichinose [a]**

[a] Research Center for Macromolecules and Biomaterials, National Institute for Materials Science, 1-1 Namiki, Tsukuba 305-0044, Japan

[b] Graduate School of Science and Technology for Innovation, Yamaguchi University, 2-16-1 Tokiwadai, Ube, Yamaguchi 755-8611, Japan

[c] Center for Advanced Materials, Forestry and Forest Products Research Institute, 1 Matsunosato, Tsukuba, Ibaraki 305-8687, Japan

*Email: ICHINOSE.Izumi@nims.go.jp

KEYWORDS: Sulfonated poly(ether sulfone), polymer-based membranes, membrane ionic conductivity, membrane permselectivity, cation exchange membranes.

Abstract

Sulfonated poly(ether sulfone) (S-PES) was synthesized through the post-sulfonation of poly(ether sulfone) (PES) with chlorosulfonic acid as the sulfonating agent. The degree of sulfonation (*DS*) of the produced S-PES was controlled between 13.2 and 36.2% by adjusting the reaction time. The *DS* values were determined by elemental analysis, ^{1}H-NMR, and titration against 0.01 M NaOH. The presence of sulfonic acid groups was confirmed using ^{1}H-NMR and FT-IR analyses. The produced S-PES with different *DS* values were cast into membranes. The performance of these materials as cation-exchange membranes (CEMs) was evaluated in detail, in light of their ion exchange capacity, water uptake, hydration number, charge density, contact angle, thermal and long-term stability, ionic conductivity, and permselectivity. The properties of the obtained membranes were compared to various reported CEMs, including industrial benchmarks such as Nafion-117, Fuji CEM, FKS-20, CMX, and CSE. We demonstrate that our work achieved the best balance between ionic conductivity and permselectivity through finely controlled *DS* optimization. The best-performing membrane was found to have a *DS* of 32.4% with a significantly high ionic conductivity of 16.85 mS cm^{-1} and a high permselectivity of 98.0% in 0.5 M NaCl. Our work sheds light on the crucial interplay between various membrane properties as the degree of functionalization stepwise varies. The fabricated membranes are promising candidates for advancing electrodialysis-based desalination and salinity-driven renewable energy production technologies.

1. Introduction

Ion exchange membranes (IEMs) play a significant role in the advancement of numerous applications, including water treatment, industrial separation, and power generation, with a focus

on selective ion dialysis, electrodialysis (ED), reverse electrodialysis (RED), and fuel cells [1–3]. The performance of ion exchange membranes (IEMs) is generally governed by their physical and electrochemical properties, such as their area resistance (*AR*), permselectivity (α), ion exchange capacity (*IEC*), water uptake (*WU*) or swelling degree (*SD*), thickness (*L*), and fixed charge density (C_{fix}). The majority of commercially available IEMs are manufactured as homogeneous membranes using functionalized polymeric materials. These commercial membranes exhibit an *AR* ranging from 1 to 5 Ω cm², an α above 90%, an *IEC* between 1.1 and 2.5 meq g^{-1}, a *WU* up to 30%, and a thickness varying from 30 to 200 μm [4–6]. As shown later in a comprehensive comparison of many reported membranes, Nafion-117 remains the best amongst the commercial membranes with 100% permselectivity and ionic conductivity of 11.6 mS cm^{-1} (1.73 Ω cm²). It is challenging to improve all these properties concomitantly due to a trade-off paradox: all these properties are strongly related and sometimes undermine each other. For example, increasing the functional groups in the polymer backbone may make it possible to produce IEMs with high ion exchange capacity and improved ionic conductivity; however, these membranes may also have low permselectivity, poor mechanical stability, low fixed charge density, and high swelling degree [7,8]. Therefore, it is worthwhile to investigate and understand the interplay between these opposing characteristics via optimizing the degree of functionalization to develop appropriate ion exchange membranes with outstanding performance.

Among the polymer materials used for IEM fabrication, S-PES is a highly promising membrane material because of its chemical and thermal durability, exceptional mechanical properties resulting from its aromatic backbone, high ionic conductivity facilitated by the high concentration of sulfonic acid groups (which could be controlled by reaction conditions), and cost efficiency [9–12]. Generally, S-PES can be produced by pre- or post-sulfonation of commercially available PES.

Owing to its low cost and ease of application, post-sulfonation is more frequently employed than pre-sulfonation. Thin membranes can be especially attractive since the decrease in membrane thickness can lead to a decrease in membrane resistance, giving rise to improved performance and reduced materials cost.

To the best of our knowledge, despite the wide literature existing on S-PES as a CEM, the crucial interplay between different polymer structures and the effect on the membrane's ionic conductivity (or permselectivity) has not been explored. Insufficient sulfonation can restrict the overall ionic conductivity, while excessive sulfonation can bring on low membrane performance, as previously mentioned [13]. CEMs of S-PES with different *DS* were previously reported by Klaysom *et al.* [8], who controlled *DS* by varying the reagent ratios. They achieved a high ionic conductivity of 29.7 mS cm^{-1} but with a very low permselectivity of 13.6%. When they achieved a high permselectivity of 95.2%, the ionic conductivity was only 0.06 mS cm^{-1}. Avci *et al.* [6] fabricated two S-PES membranes (sPES-D and sPES-P) using commercial S-PES (Konishi Co., Japan). The reported ionic conductivity was 5.73 and 18.86 mS cm^{-1} with a permselectivity of 95.0 and 84.0%, respectively. The high ionic conductivity has not been achieved without lowering the permselectivity. Cassady *et al.* [14] and Rochow *et al.* [15] used commercial S-PES (YANJIN Technology, Tianjin, China) with *DS* from 20 to 60% and reported high permselectivity values (91.1 – 100%). Membrane with *DS* of 50% was found to have an ionic conductivity of 3.13 mS cm^{-1} (area resistance = 0.67 Ω cm^2), with a permselectivity of 95.4%. Komuta *et al.* [16] have reported a series of S-PES membranes for dialysis applications. The best achieved balance between ionic conductivity and permselectivity was 3.66 mS cm^{-1} (*AR* = 1.03 Ω cm^2) and 98.0%. Furthermore, Rezayani *et al.* [17] extensively performed molecular dynamics (MD) simulations on S-PES membranes with various *DS* values to correlate some membrane morphological parameters,

such as normalized water cluster size, pore limiting diameter (PLD), and water residence time, to the water/ion diffusion behavior.

All these previous studies on S-PES as a CEM have not reported an optimal *DS* range; that is, the best balance between ionic conductivity and permselectivity was not achieved. Investigating the optimal *DS* value for S-PES is not only a modification of the same structure but also a regulation of several morphological key parameters that affect water and charge transfer through the membrane.

Therefore, in this work, we addressed the fine-tuning in *DS* for S-PES as CEMs by controlling the reaction time. We investigated the trade-off between ionic conductivity, permselectivity, and other membrane physical properties to find the optimal *DS* and the best performance as a CEM. This could open more prospects and insights for various membrane-based technologies, such as water desalination by ED, sustainable energy production using RED, and fuel cells.

2. Experimental

2.1. Materials

Poly(ether sulfone) (SumikaExcel PES 7600P) was purchased from Sumitomo Chemical Company (Tokyo, Japan), and dried at 90 °C under vacuum for 24 hours before use. 1-Methyl-2-pyrrolidinone (NMP; CAS No. 872-50-4, 99%), chlorosulfonic acid (CAS No. 7790-94-5, 97%), sulfolane (CAS No. 126-33-0, 95%) that was dehydrated using molecular sieves for 24 hours before use (4A, Sigma Aldrich Co.), analytical grade sodium chloride (CAS No. 7647-14-5), sodium hydroxide (CAS No. 1310-73-2), potassium chloride (CAS No. 7447-40-7) and

phenolphthalein (CAS No. 77-09-8) were all purchased from FUJIFILM Wako Pure Chemical Corporation (Osaka, Japan). CSE Neosepta was purchased from ASTOM Corp., Japan.

2.2. Sulfonation reaction

10.6 g of PES was stirred with 60 g of sulfolane in a three-neck flask until complete dissolution. 15.6 g of chlorosulfonic acid was added dropwise over 30 minutes. Then the reaction mixture was refluxed under a nitrogen atmosphere at 100 °C in an oil bath [18]. Sampling was done every 2 hours up to 24 hours, and the solution was poured into deionized water. The precipitated polymer pellets were washed with deionized water several times until a neutral pH was reached and dried at 70 °C under vacuum for 24 hours. This drying process was repeated each time prior to use.

2.3. Membrane preparation

The dried S-PES pellets were dissolved in NMP to form a 5% (w/v) polymer solution, and then a suitable amount of the polymer solution was cast onto a glass surface. S-PES membrane was obtained by drying the casting solution at 70 °C for 2 days in a vacuum oven. The membrane adsorbs water slowly, so that it was further dried at 70 °C for 24 hours in a vacuum oven before characterization.

2.4. Characterization of S-PES

2.4.1. FT-IR

FT-IR spectra were recorded on dried S-PES and PES membrane samples using a JASCO FTIR-6200 spectrophotometer equipped with an ATR accessory (ATR PRO450-S, JASCO, Japan). Measurements were done with a resolution of 4 cm^{-1}, and 32 scans were collected and averaged. Nitrogen gas purge was performed before the analysis.

2.4.2. Scanning electron microscopy (SEM) and elemental analysis

Scanning electron microscopy images were recorded using an SEM SU5000 apparatus (Hitachi, Japan). Sulfur content was determined through energy dispersive X-ray spectroscopy (EDX) by means of an EDX probe (AMETEX-30491, USA). *DS* values were calculated according to the following equation (Eq. 1):

$$DS\ (\%) = \frac{M-T}{H} \times 100 \quad (1)$$

, where *M* is the measured S/C atomic% in the S-PES sample, *T* is the theoretical S/C atomic% in PES (8.33%), and *H* is the maximum increase in the S/C% in the case of 100% *DS* (also 8.33%). Here, we assume one sulfonic acid group per monomeric unit for full (100%) substitution.

2.4.3. ^{1}H-NMR

Proton nuclear magnetic resonance (^{1}H-NMR) spectra were obtained using a JEOL AL 400 (400 MHz, 9.38T) apparatus with deuterated dimethyl sulfoxide (DMSO-d_6) as the solvent. All samples were dried overnight at 60 °C under vacuum before the measurement. The samples were dissolved in DMSO-d_6 under an Ar atmosphere. All the data are given as chemical shifts in δ (ppm) relative to $(CH_3)_4Si$.

DS of S-PES was calculated based on the integral peak values of the obtained spectra using the following equations (Eq. 2 and Eq. 3) [19]:

$$z = \frac{AH_E}{\sum AH_{A,B,C,D}} \quad (2)$$

$$DS\ (\%) = \frac{8z}{1+2z} \times 100 \quad (3)$$

, where AH_E is the integral peak value for H_E, and $\sum AH_{A,B,C,D}$ is the integral for H_A, H_B, H_C, and H_D (see Fig. S3).

2.4.4. Thermal gravimetric analysis (TGA)

The thermal stability of PES and S-PES was investigated using a thermal gravimetric analysis apparatus (STA200RV, Hitachi, Japan) under a nitrogen gas flow of 200 mL min^{-1} with a heating rate of 10 °C min^{-1} in the temperature range of 25 – 600 °C. 10 mg sample was dried at 60 °C under vacuum for each measurement.

2.5. Ion exchange capacity

Ion exchange capacity (*IEC*) is defined as milliequivalents of sulfonic acid groups per gram of dried membrane. *IEC* was determined by acid-base titration using 0.01 M NaOH. In the first step, the membrane sample was immersed in 1.0 M HCl for 48 hours to ensure that all the negatively charged sulfonic acid groups were saturated with protons. Then, the membrane was rinsed with deionized water and immersed in 2.0 M NaCl solution for 48 hours to replace all protons with sodium ions. This step was repeated two times to ensure that all the protons within the membrane matrix were released into the solution. Finally, all the NaCl solutions were collected and titrated against 0.01 M NaOH using a phenolphthalein indicator. *IEC* was calculated using the following equation (Eq. 4):

$$IEC\ (meq\ g^{-1}) = \frac{C \times V}{w_{dry}} \tag{4}$$

, where C (mM) is the concentration of NaOH solution (0.01 M), V (L) is its volume consumed during titration, and w_{dry} (g) is the mass of the dry membrane.

DS is defined as the number of sulfonic acid groups per repeating unit of polymer. It was calculated from the *IEC* value using the following equation (Eq. 5) [20,21]:

$$DS\ (\%) = \frac{\left[\left(\frac{IEC}{1000}\right) \times M_{wt}\ (\mathrm{RU})\right]}{1 - \left[\left(\frac{IEC}{1000}\right) \times M_{wt}\ (SO_3)\right]} \times 100 \tag{5}$$

, where M_{wt} (RU) and M_{wt} (SO_3) are the molecular weights of the repeating unit and the pendant SO_3 group wit values of 232 and 81 g mol^{-1}, respectively.

2.6. Water uptake

Water uptake (*WU*) is defined as the weight of absorbed water in grams per gram of the dried membrane. To calculate *WU*, each membrane was dried for 24 hours at 70 °C in a vacuum oven and then immersed in deionized water for 48 hours at room temperature. *WU* was calculated according to the following equation (Eq. 6):

$$WU\ (\%) = \frac{w_{wet} - w_{dry}}{w_{dry}} \times 100 \quad (6)$$

, where w_{wet} and w_{dry} are the masses of the wet and dried membranes in grams, respectively.

2.7. Hydration number

Hydration number (λ) is defined as the number of water molecules per ionic sulfonate group, and can be calculated according to the following equation (Eq. 7) [21]:

$$\lambda = \frac{1000\ (w_{wet} - w_{dry})}{18 \times w_{dry} \times IEC} \quad (7)$$

2.8. Fixed charge density

Fixed charge density (C_{fix}) is defined as mmol (or meq) of fixed charged groups per gram of absorbed water, and was calculated using *IEC* and *WU* values according to the following equation (Eq. 8) [7,22]:

$$C_{fix}\ (\text{meq}\ g^{-1}_{water}) = \frac{IEC}{WU\%} \times 100 \quad (8)$$

2.9. Contact angle

The contact angle (*CA*) of water on PES and S-PES membranes was measured at room temperature using a contact angle measurement instrument (DMe-211 Plus; FAMAS software, Kyowa, Osaka, Japan). Five angles were measured in different places on the membrane surface, and the average value was taken.

2.10. Mechanical strength

A tensile tester (Autograph AGS-X, Shimadzu, Japan) was used to investigate the mechanical strength of dry and wet membranes at room temperature. The PES and S-PES (with different *DS*) membrane samples were pulled at 1.0 mm min^{-1} crosshead speed. Membranes with dimensions of 15 × 10 mm and a thickness of 0.07 mm were prepared for the tensile test. Samples were dried at 70 °C for 24 hours under vacuum for the dry state measurements, and then immersed in deionized water for 24 hours for the wet state measurements. The membrane thicknesses were measured using a Niigata Seiki SK Micrometer Stand S-Type 25-100 MS-SG, Japan.

2.11. Ionic conductivity measurement

The membrane resistance was determined by applying an alternating current (AC) at a frequency of 10 kHz to a two-compartment cell filled with 0.5 M NaCl aqueous solution [22,23], as shown in Fig. 1a, using an LCR meter (DE-5000, Taiwan). Each membrane was immersed in 0.5 M NaCl for 24 hours before measurement. The solution was circulated using an external feed pump with a flow rate of 100 mL min^{-1} at 25 ± 0.1°C. The two compartments were connected to the LCR meter with two fixed platinum electrodes that remained in the same position for all measurements. The membrane resistance (R_m, Ω) was calculated by subtracting the resistance of the blank (no membrane present). The area resistance can be obtained by dividing R_m by the effective area of the membrane (A, 0.949 cm^2). The membrane ionic conductivity (σ, S cm^{-1}) was calculated using the following equation (Eq. 9):

$$\sigma\ (S\ cm^{-1}) = \frac{L}{R_m A} \tag{9}$$

, where L is the thickness of the membrane (cm).

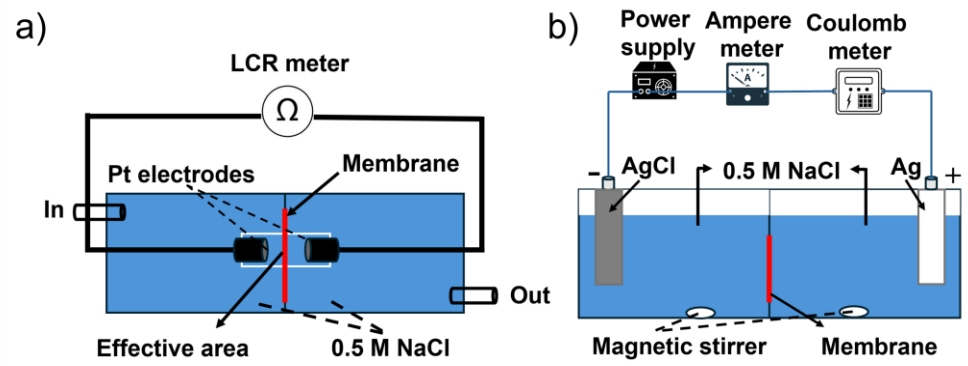

Figure 1. Schematic diagram of the measurement setup for determining membrane ionic conductivity (a) and permselectivity (b).

2.12. Permselectivity measurement (Hittorf method)

The membrane permselectivity was determined by means of the dynamic state ion transport number (t_{d+}) as an indicator of the counter-ion permselectivity for IEMs [23,24]. Therefore, the permselectivity term (α) will be used in our study to refer to the counter-ion selective permeation through the membrane. The measurement was carried out using a two-chamber cell as shown in Fig. 1b. A direct current with a current density of 10 mA cm^{-2} was applied between the two Ag and AgCl electrodes in a two-chamber cell containing 0.5 M NaCl at 25 °C [22]. After the experiment, the conductivity difference between the two chambers was measured to determine the corresponding concentration change caused by ion transport via the membrane. The following equation was used to determine the dynamic state ion transport number (Eq. 10):

$$\alpha\ (\%)\ = t_{d+} = \frac{\Delta m \times V \times F}{Q} \times 100 \qquad (10)$$

, where Δm, V, F, and Q are the equivalent change in ions, solution volume (L), Faraday constant (96485 C mol^{-1}), and electric charge (C) flowing across the membrane during the test, respectively.

3. Results and discussion

3.1. Sulfonation reaction

Sulfonation of PES is basically a second-order bimolecular aromatic electrophilic substitution reaction (PES + $ClSO_3H$ → S-PES + HCl) that obeys the second-order rate law according to the following equation (Eq. 11) [25,26].

$$\frac{dc}{dt} = k\,(a-c)(b-c) \tag{11}$$

, where *a* and *b* are the initial concentrations of PES and chlorosulfonic acid (M), respectively. *c* is the concentration of the produced S-PES at time *t*. *k* is the reaction rate constant ($M^{-1}\ h^{-1}$)

From Eq. 11, the following equation is obtained (Eq. 12) [25].

$$\frac{1}{a-b} ln \frac{b(a-c)}{a(b-c)} = kt \tag{12}$$

The reaction rate (followed by the change in *DS* with time) was found to obey Eq. 12, with a correlation coefficient of 0.992 as shown in Fig. S1a. The rate constant was calculated to be 2.48 $\times 10^{-2}\ M^{-1}\ h^{-1}$.

Generally, electron-withdrawing groups deactivate the aromatic ring for sulfonation. Since the sulfone linkage in PES is an electron-withdrawing substituent, the sulfonation reaction was regarded to take place only at the meta position to the sulfone linkage, that is ortho position to the ether linkage in PES. As previously reported by Hu *et al.*[27] , who performed a molecular simulation for the sulfonation site during similar reaction, indicating the feasibility of the attack on the meta position with respect to the sulfone linkage due to the lower activation energy of its transition state while the other sites adjacent to the bulky sulfone linkage is hindered by steric repulsion and hence have a higher activation energy. The introduction of the strong electron-withdrawing sulfonic acid group further deactivates the aromatic ring towards sulfonation. Thus, on average, one sulfonic

acid group per monomeric unit can usually be introduced into the PES backbone at position meta to the sulfone group adjacent to the ether linkage, as we show in Fig. 2a [28]. Therefore, PES with only one of the protons substituted by the sulfonic acid group was considered as the product.

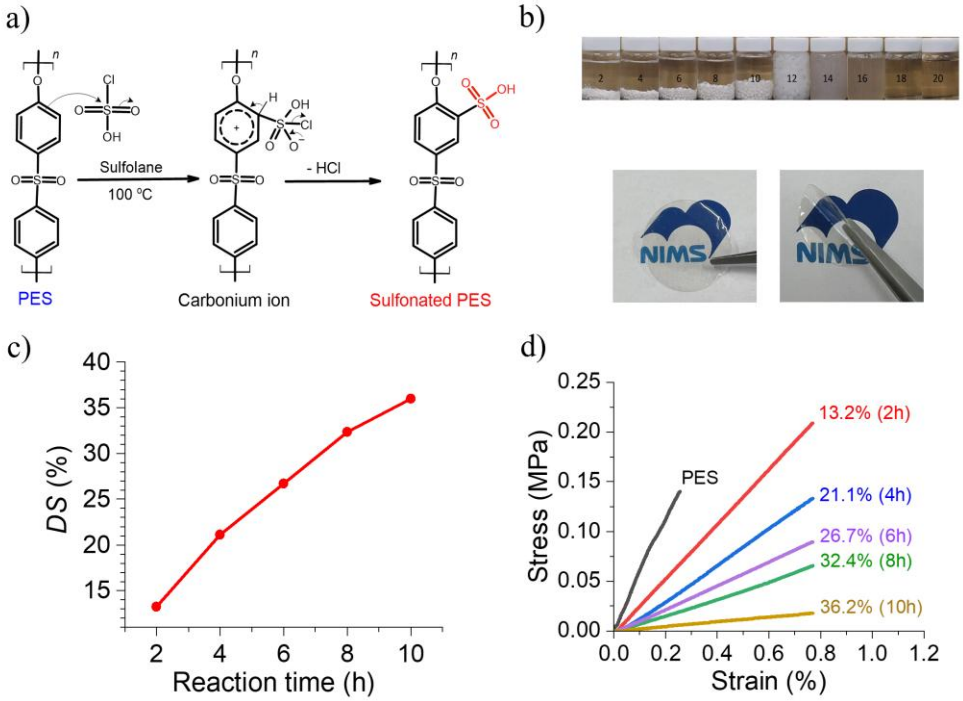

Figure 2. (a) Sulfonation reaction mechanism for PES, (b-top) appearance of the precipitated S-PES pellets at different reaction times/hour, after immersion in deionized water for 7 days, (b-bottom) appearance of the flat and bent S-PES membranes with a *DS* of 36.2%, (c) *DS* of the produced S-PES at different reaction times, (d) stress-strain curves for PES and S-PES membranes with different *DS* in the dry state.

DS values for the produced S-PES were calculated based on three techniques: (a) measuring the percentage of sulfur in a dry sample using EDX elemental analysis according to Eq. 1, (b) using the integral peak values in the ^{1}H-NMR spectra based on Eq. 2 and Eq. 3, and (c) using *IEC* values calculated from the titration experiment according to Eq. 5. The values of *DS* using the three

techniques as well as the average values as a function of the reaction time are shown in Table S1 and Fig. 2c. Since the three methods have a certain experimental error, we used the mean average values without any weighing for the discussion on *DS*.

When the reaction time was 2-10 hours, similar precipitated pellets were formed. However, the pellets produced by longer reaction times tend to swell after being kept in deionized water. As shown in Fig. 2b, the pellets produced by 12 hours reaction time were largely swollen in deionized water after immersion for 7 days. After 14 days of water immersion, this sample completely dissolved in deionized water, as well as other samples produced in longer reaction times (Fig. S1b). Probably, S-PES with a high *DS* value behaves as a polymer surfactant and slowly forms a colloidal dispersion in deionized water.

The produced S-PES membranes have been characterized using SEM (Fig. S2), FT-IR (Fig. 4a), ^{1}H-NMR (Fig. S3), and TGA-DTA (Fig. S4) to confirm the membrane morphology, chemical structure, and thermal stability, respectively.

3.2. Physical and electrochemical properties of S-PES membranes

3.2.1. Basic physical properties

IEC, *WU*, C_{fix}, and *CA* are crucial parameters ultimately governing the ionic conductivity and permselectivity of IEMs. These basic physical properties are summarized in Table 1 as a function of reaction time and *DS*. *IEC* and *WU* monotonously increase with increasing *DS*, with a concomitant decrease in C_{fix}, in line with general expectations. As the number of SO_3H groups increases, the membranes become more hydrophilic. This trend can be confirmed by the decreasing water contact angle from 95.6° for PES to 50.5° for S-PES after 10 hours of reaction time (Fig. 3a). The hydration number was also found to be increasing with *DS* due to the increased largest

cavity diameter (*LCD*), giving a larger space for more water molecules to surround the sulfonate groups [17]. The *IEC* value in case of *DS* = 0% (for PES), is due to the fact that the membrane itself absorbed a small amount of the solutions during the titration experiment, and not due to the presence of any ion exchange groups. So, this value can be neglected.

3.2.2. Mechanical strength

Because the fabricated S-PESs are targeted to be used in membrane-based technologies, especially for ED and RED, investigating the mechanical properties in both dry and wet states is imperative. In the dry state, the mechanical strength and elongation at break decrease for the S-PES membranes compared to the pure PES membrane (Fig. 3c and d). This may be explained by the random introduction of the highly polar sulfonic acid groups into the PES chain, generating inhomogeneities along the polymer backbone. The configuration of the polymer chains also expands with the introduction of sulfonic acid groups, hindering entanglement formation and weakening primary intermolecular interactions (such as π stacking) [29]. As shown in Fig. 3c and d, the wet S-PES membranes exhibit a much lower tensile strength and higher elongation at break (by around 0.9 and 6 times, respectively) compared to dry ones. The polymeric chains are plasticized by the absorbed water molecules, resulting in an increase in their segmental mobility, significantly affecting their mechanical response [29]. Moreover, the elongation of the wet S-PES membranes decreases with increasing *DS*, as in the case of higher *DS*, the membranes are more swollen due to the higher water uptake, and further elongation will be more difficult. The elastic modulus of PES and S-PES membranes at the dry and wet state (Fig. 3b) was calculated from the stress-strain curves shown in Fig. 2d and Fig. S5a, respectively.

Table 1. Basic properties of the fabricated PES and S-PES membranes as a function of the reaction time and *DS*.

Reaction time (h)	*DS* (%)	*IEC* (meq g^{-1})	*WU* (%)	C_{fix} (meq g_{water}^{-1})	*CA* (°)	λ
0	0	0.08	1.2	6.8 ± 1.0	95.6	0
2	13.2	0.61	5.7	10.8 ± 0.8	94.4	5
4	21.1	0.90	10.0	9.0 ± 0.1	91.3	6
6	26.7	1.03	16.1	6.4 ± 0.7	70.1	9
8	32.4	1.29	20.6	6.3 ± 0.4	63.7	9
10	36.2	1.36	26.3	5.2 ± 0.3	50.5	11

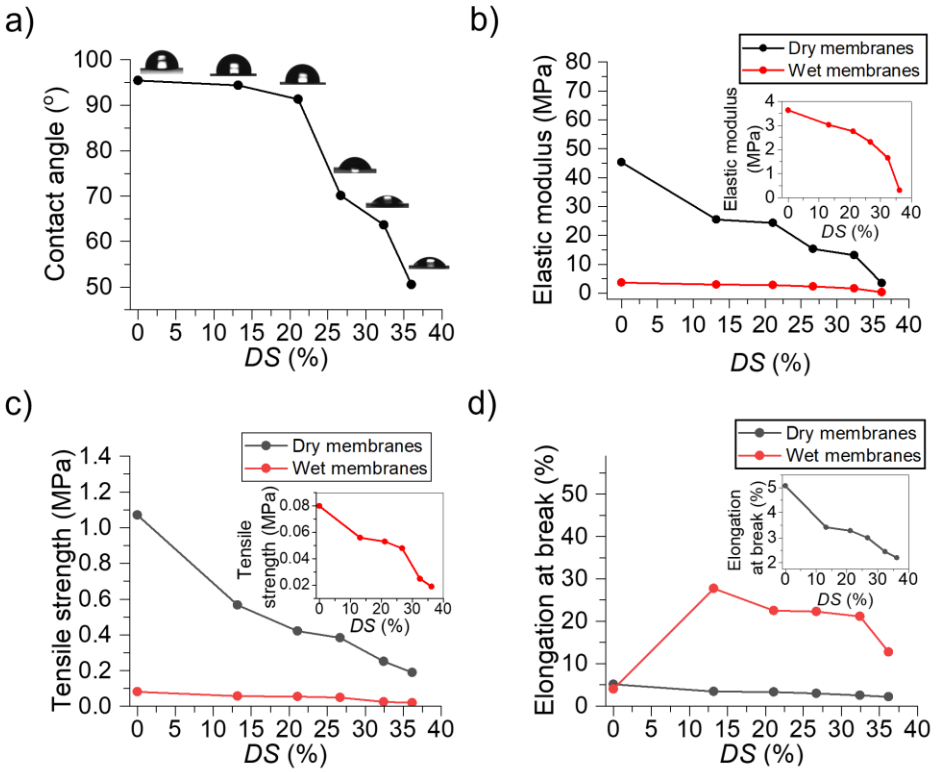

Figure 3. (a) Water contact angles of PES and S-PES membranes with different *DS*, (b) elastic moduli of the dry and wet PES and S-PES membranes with different *DS* (inset shows the elastic modulus of the wet membranes), (c) tensile strength of the dry and wet PES and S-PES membranes with different *DS* (inset shows the tensile strength of the wet membranes), (d) elongation at break

of the dry and wet PES and S-PES membranes with different *DS* (inset shows the elongation at break of the dry membranes).

3.2.3. Long-term stability

The membrane's long-term and thermal stabilities were confirmed using FT-IR, as shown in Fig. 4, in which S-PES membrane sample (*DS* = 36.2%, 10 h reaction time) was immersed in 0.5 M NaCl at room temperature for more than 120 days, then rinsed with deionized water and dried at 60 °C for 24 hours before the measurement (Fig. 4a). Additionally, the stability of S-PES membranes with different *DS* values in 0.5 M NaCl at 50 °C for 14 days was tested as shown in Fig. 4b. Neither membrane was dissolved nor swollen after the experiment. These results confirm the stability of the membrane at 25 and 50 °C. The intensity of the characteristic peak for the SO_3H group at 1025 cm^{-1} is increasing with reaction time. We also confirmed that no change in these peaks was observed after immersion at 50 °C for 14 days. The surface and cross-sectional photo images of the S-PES membrane in Fig. 4c (*DS* = 36.2%, 10 h reaction time) confirm that no surface morphological change occurs after stirring in 0.5 M NaCl for 14 days at 50 °C. When the temperature was raised to 70 °C, this membrane dissolved. S-PES membrane with *DS* of 32.4% (8h reaction time) also dissolved in the same condition, indicating the maximum possible operating temperature at high *DS* values (above 30%) is less than 50 °C. S-PES membrane with *DS* of 27.1% (6h reaction time) was still stable at 70 °C. Note that the S-PES membrane (8h) is slightly swollen in a 10% methanol solution; these membranes are not stable in water/alcohol mixtures.

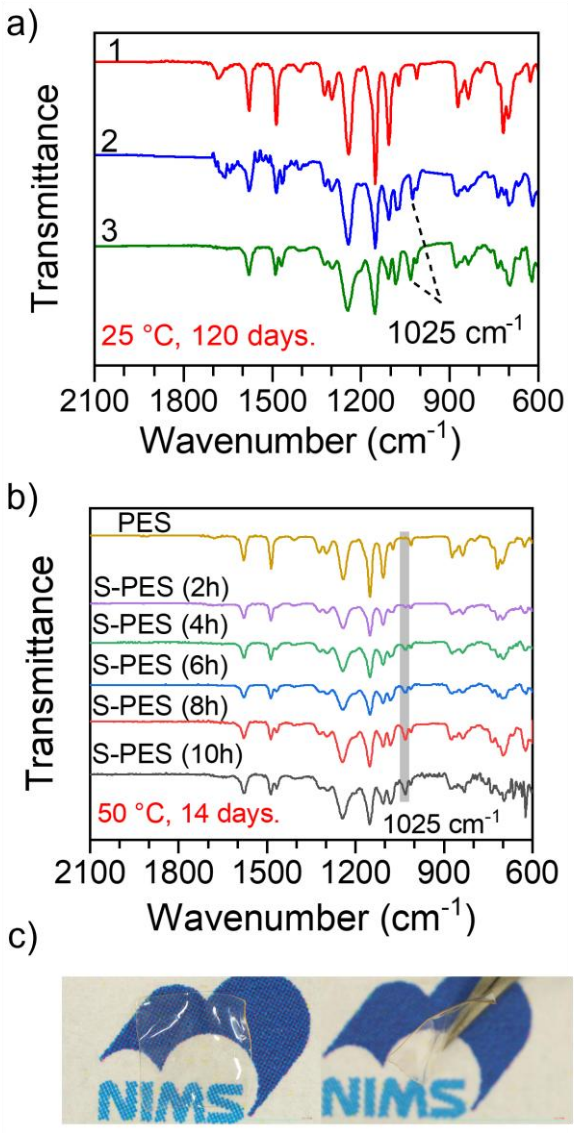

Figure 4. (a) FT-IR spectra for (1) PES,(2) pristine S-PES, and (3) S-PES after immersion in 0.5 M NaCl for 120 days, (b) FT-IR spectra for PES and S-PES produced at different reaction times after stirring in 0.5 M NaCl for 14 days at 50 °C, (c) surface and cross-sectional images of S-PES membrane (DS= 36.2%) after stirring in 0.5 M NaCl for 14 days at 50°C.

3.2.4. Membrane ionic conductivity

The membrane ionic conductivity is one of the principal parameters for the performance of IEMs. Generally, the presence of ion exchange groups within the membrane matrix is one of the main

factors that determines the *WU* and ionic conductivity of IEMs. It is expected that with increasing *IEC,* the *WU* and membrane ionic conductivity will concomitantly increase. In addition to *IEC*, there are some factors affecting *WU* that have to be taken into consideration, such as polymer hydrophilicity and membrane morphology [30–32]. The right balance between all these parameters is very important to achieve an outstanding performance [4].

The ionic conductivity of the fabricated S-PES membranes as a function of *DS* and reaction time is shown in Fig. 5a. The corresponding area resistance values derived from the same experiments are shown in Fig. S5b. The membrane ionic conductivity increases up to 25.34 mS cm^{-1} with increasing *DS* to 36.2% (10 hours reaction time). Rezayani *et al.* noted that when the hydration number was 10 for S-PES with *DS* of 30 and 40%, the water networks within the polymer matrix were almost interconnected, resulting in a high diffusion rate [17]. At this stage, the pore limiting diameter (*PLD*) also started to exceed the diameter of the water molecule (0.32 nm). As the *PLD* exceeded the critical diameter with higher *DS*, it could be expected that both small cations and the large water molecule would permeate through the membrane, and permselectivity would decrease. In our study, the hydration number was 9 and 11 for our prepared membranes at *DS* 32 and 36%, respectively. As we have shown, *DS* of 32% provided the best balance of ionic conductivity and permselectivity, which has a hydration number close to the reported value by Rezayani *et al.*

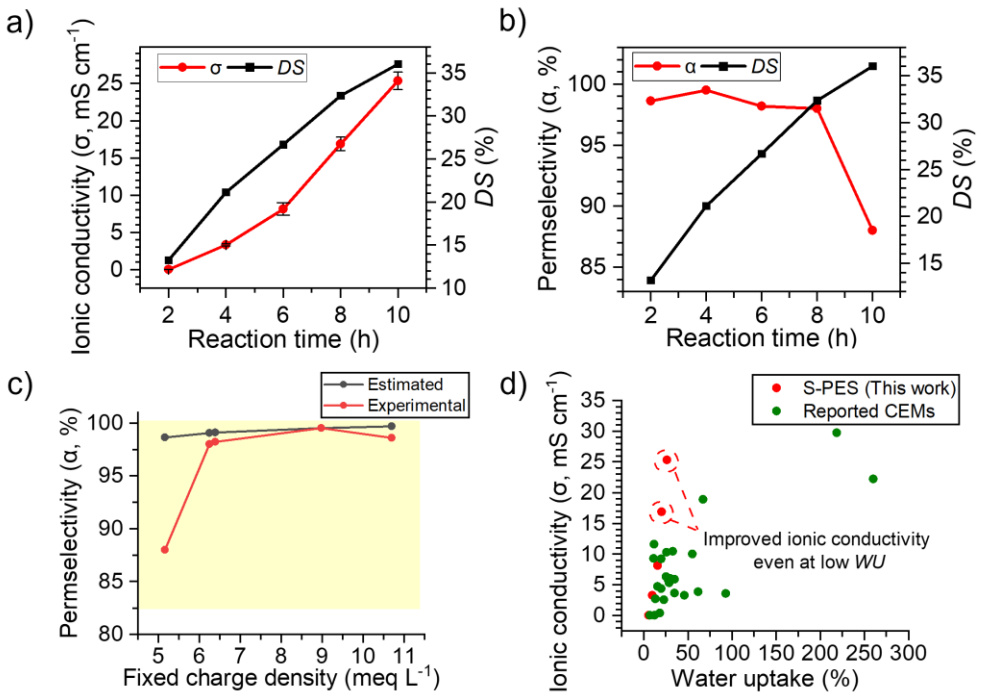

Figure 5. (a) Ionic conductivity and (b) permselectivity of the fabricated S-PES membranes as a function of reaction time, (c) estimated and experimental permselectivity of the different S-PES membranes as a function of the fixed charge density (yellow region is the permselectivity range of commercial CEMs in Table 2), (d) ionic conductivity of S-PES and previously reported CEMs as a function of water uptake.

3.2.5. Membrane permselectivity

The permselectivity of a membrane is defined as the flux of an individual element in comparison to the total flux through the membrane under a certain driving force [7]. The permselectivity of IEMs is a measure of how well the membrane can distinguish between anions (such as Cl^-) and cations (such as Na^+) [7]. Similar to membrane ionic conductivity, membrane permselectivity is also an essential factor determining the membrane performance.

Regarding permselectivity, C_{fix} exerts one of the most prominent impacts on this property [6,7,22]. For example, a high *IEC* will not surely indicate high permselectivity, as the membrane may have

a high *WU,* leading to a low C_{fix} and weaker exclusion of co-ions. As a result, the permselectivity value may be lower than expected. However, it is possible to produce membranes with a higher permselectivity by increasing *IEC* if the *WU* is well controlled [33].

The permselectivity of the prepared S-PES membranes as a function of reaction time is shown in Fig. 5b. As mentioned before, the higher the C_{fix}, the stronger the exclusion of co-ions and the higher the permselectivity. As presented in Table 1, there is a larger increase in *WU* with increasing *DS* compared to the *IEC* values. Therefore, C_{fix} decreases with time in line with Eq. 8. Thus, it can be noticed that for the higher C_{fix} values (10.8 - 6.3 meq g_{water}^{-1}), the S-PES membranes show comparable permselectivity values between 98.0 and 99.0%. At a C_{fix} of 5.2 meq g_{water}^{-1}, the permselectivity of the membrane decreases to 88.0%. This can give an indication on the boundary line where the decrease in C_{fix} results in a significant decline in permselectivity for S-PES membranes.

Also, another reason for the decreasing permselectivity lies in the increased *WU*, providing higher ionic mobilities for the co-ions due to higher free water content. An increased volume of free water within the membrane can result in greater space for co-ions to pass through the membrane with less friction between the ions and the membrane polymer, as well as among the ions themselves (solute-membrane and solute-solute friction) [34].

The permselectivity of the counterion (Na^+ in case of NaCl solution) through the ion exchange membrane can be theoretically estimated using the following equation [22]:

$$\text{Estimated permselectivity} = \frac{ú_{Na}\left[\left(\sqrt{{C_{fix}}^2+4C^2}\right)+C_{fix}\right]}{ú_{Na}\left[\left(\sqrt{{C_{fix}}^2+4C^2}\right)+C_{fix}\right]+ ú_{Cl}\left[\left(\sqrt{{C_{fix}}^2+4C^2}\right)-C_{fix}\right]} \quad (13)$$

, where $\acute{u}_{Na}$ and $\acute{u}_{Cl}$ are the ionic mobilities of Na^+ and Cl^-, respectively ($\acute{u}_{Na}/\acute{u}_{Cl} = 0.656$) [14,35]. C is the concentration of NaCl solution (0.5 mol L^{-1}).

Using the above equation, the permselectivity values for S-PES membranes with different *DS* can be theoretically estimated as a function of C_{fix} and compared to the experimental ones as presented in Fig. 5c. As concluded from the figure, the experimental and theoretical values are in strong agreement with each other, ranging from 98.0% to 99.6%, except for the membrane with the lowest C_{fix} of 5.2 meq g_{water}^{-1}, which has a *DS* of 36.2%. This may be explained by the heterogeneity of the fixed ion concentration at high *WU* compared to the other S-PES membranes with lower *DS* [22,36].

3.2.6. Trade-off between ionic conductivity and permselectivity

A detailed understanding of the complex interplay among *IEC*, *WU*, and C_{fix} is crucial for the development of an IEM with high ionic conductivity and permselectivity as discussed above. Table 2 shows a comparison between S-PES membranes in this work and various CEMs reported in literature. One of the outstanding merits of the S-PES membranes in this study is the high ionic conductivity without absorbing too much water and thus, without compromising the permselectivity, compared to various reported CEMs, as shown in Fig. 5d and Fig. S6b. As a result, the essential balance in the trade-off between ionic conductivity and permselectivity is achieved. It can be concluded that the fabricated membrane using S-PES with a *DS* value of 36.2% (10 hours reaction time) shows the highest ionic conductivity value of 25.34 mS cm^{-1}, and the lowest permselectivity value of 88.0% compared to the other S-PES membranes fabricated with shorter reaction times (2-8 hours). Whereas the membrane with a *DS* of 32.4% (8 h reaction time) provides a good balance in the trade-off between these properties, with a significantly high ionic

conductivity of 16.85 mS cm^{-1} (an area resistance of 0.49 Ω cm^2) and high permselectivity of 98.0%. Therefore, among the membranes fabricated in this work, we see S-PES with a *DS* of 32.4% (8 h reaction time) as a promising CEM with the best sulfonation-controlled trade-off between ionic conductivity and permselectivity, as compared to previous studies on S-PES that have been discussed in detail in the introduction section.

For direct experimental comparisons and performance validation, CSE, Neosepta (ASTOM Corp., Japan) has been used for side-by-side evaluation. Additionally, in our previous work by Sugimoto *et al*. [37], the performance evaluation of some leading commercial membranes, such as CMX, CIMS, and C-2 (ASTOM Corp., Japan), as well as FKS-20 (FUMATECH BWT GmbH, Germany), has been conducted using the same setups and under the same conditions as our S-PES membranes, so we also used these data for direct comparisons. Fig. 6 shows the performances of the best reported membranes from Table 2, including those from the side-by-side evaluation. The best commercial membrane, Nafion-117, has 100% permselectivity and 11.61 mS cm^{-1} ionic conductivity. Our best membrane with *DS* of 32% has a comparable permselectivity of 98% but ionic conductivity is 45% higher than that of Nafion-117. Fuji CEM-1 has even lower permselectivity and ion conductivity of 92% and 10 mS cm^{-1}, respectively.

Avci *et al*. reported the performances of CEMs made of commercial S-PES (Konishi Co., Japan) with an IEC value of 1.19 meq g^{-1} and showed a power density output of 3.92 W/m^2 for 0.1/4.0 M NaCl at 25 °C in RED [6]. Therefore, the power density output of our optimum membrane may largely exceed this value, since the resistance of our membrane is just 45% of this membrane. Of course, this is the case in which CEM resistance is the major factor in the total resistance of the RED setup. In the practical application, it is not easy to achieve an output higher than 5.0 W/m^2.

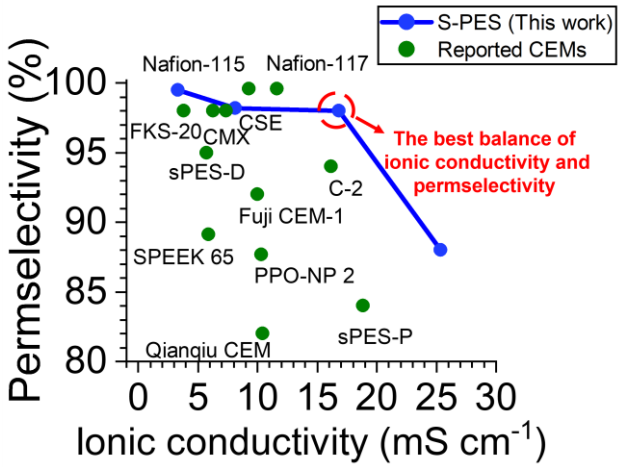

Figure 6. Ionic conductivity and permselectivity of S-PES membranes fabricated in this work compared to previously reported cation exchange membranes.

Although Nafion membranes have high performance, several drawbacks limit their future prospects. On one hand, the high production cost due to the fluorination step makes Nafion an expensive option for various technologies. On the other hand, Nafion-117 is a typical perfluorinated sulfonic acid (PFSA) membrane, which can be a potential source of many perfluorinated chemicals when used and disposed of, including the hazardous and environmentally persistent perfluoro carboxylic acids (PFCAs) [38,39]. These chemicals are currently present in human blood and are omnipresent around the world [40]. The presence of PFCAs in the environment has raised widespread concerns due to immunotoxicity, carcinogenicity, developmental and hormonal impacts based on laboratory animal toxicology investigations [41]. On the other hand, although PES-based membranes are degraded to microplastics in the long term, it is expected to decompose into harmless materials, being a better alternative from the environmental point of view [42,43]. Therefore, these functional, economic, and environmental challenges triggered research toward better alternatives.

Table 2. Comparison between the produced S-PES membranes in this work and other CEMs reported in the literature.

Membrane	*L* (μm)	*IEC* (meq g^{-1})	*WU* (%)	C_{fix} (meq g_{water}^{-1})	*α* (%)	AR^a (Ω cm^2)	σ^a (mS cm^{-1})	Ref.
S-PES (10 h)	70±10	1.36	26.3	5.2	88.0	0.41	25.34	Ours
S-PES (8h)	70±10	1.29	20.6	6.3	98.0	0.49	16.85	Ours
S-PES (6h)	70±10	1.03	16.1	6.4	98.2	0.65	8.14	Ours
S-PES (4h)	70±10	0.90	9.99	9.0	99.5	2.10	3.31	Ours
S-PES (2h)	70±10	0.61	5.67	10.8	98.6	344.50	0.02	Ours
CSE	150	-	-	-	98.0	2.14	7.15	Ours
sPES-25 (E)	80±10	0.53	7.26	7.28	88.8	278.74	0.03	[8]
sPES-40 (E)	80±10	1.44	12.5	11.45	95.2	135.36	0.06	[8]
sPES-55 (E)	80±10	1.58	18.2	8.66	80.5	18.88	0.42	[8]
sPES-25 (P)	80±10	0.73	260	0.28	13.7	0.36	22.22	[8]
sPES-40 (P)	80±10	0.60	219	0.27	13.6	0.27	29.70	[8]
sPES-P[b]	83±6	1.15	67.2	1.70	84.0	0.44	18.86	[6]
sPES-D[b]	63±6	1.19	28.0	4.30	95.0	1.10	5.73	[6]
SPES-20[b]	-	0.92	-	-	100.0	-	-	[14]
SPES-30[b]	-	1.34	-	-	99.9	-	-	[14]
SPES-40[b]	-	1.72	-	-	98.1	-	-	[14]
SPES-50[b]	21	2.08	-	-	95.4	0.67	3.13	[14, 15]
SPES-60[b]	-	2.42	-	-	91.1	-	-	[14]
SPES-CEM 1	34	0.98	13.0	1.84	97.0	1.03	3.30	[16]
SPES-CEM 6	63	1.69	7.0	1.77	98.0	1.72	3.66	[16]
Nafion-117	201±8	0.90	11.7	7.70	100	1.73	11.61	[44]

Nafion-115	139±8	0.90	11.2	8.00	100	1.50	9.26	[44]
Fuji CEM-1	120	1.96	55.0	3.60	92.0	1.20	10.00	[6]
Fuji CEM10	-	1.70	21.0	8.00	94.7	2.30	-	[45]
CIMS	150	2.30	30.0	-	98.0	2.49	6.02	[37, 46]
CMX	170	-	-	1.86	98.0	2.70	6.29	[37]
FKS-20	18	-	-	1.93	98.0	0.47	3.83	[37]
C-2	34	-	-	-	94.0	0.21	16.19	[37]
Fumasep FKD	113	1.14	29.0	-	89.5	2.14	5.28	[4,47]
Fumasep FKS	40	1.54	13.5	-	94.2	1.50	2.67	[7]
Asahi CMV	100	2.00	20.0	10.10	98.8	2.30	4.35	[7]
Asahi CSO	100	1.04	16.0	6.50	92.3	2.26	4.76	[1]
SPEEK 65	72	1.76	35.0	4.90	89.1	1.22	5.90	[7]
SPEEK 40	53	1.23	23.0	5.30	85.3	2.05	2.59	[7]
Qianqiu CEM	205	1.21	33.0	3.70	82.0	1.97	10.41	[7]
PPO-NP 1	100	1.0	20.0	5.00	84.4	1.09	9.17	[1]
PPO-NP 2	100	1.4	26.0	5.40	87.7	0.97	10.31	[1]
PPO-PVA 1	50	1.91	46.0	4.20	87.3	1.54	3.25	[1]
PPO-PVA 2	50	1.80	62.0	2.90	84.2	1.30	3.85	[1]
PPO-PVA 3	50	1.58	93.0	1.70	81.0	1.41	3.55	[1]

[a] Tested in 0.5 M NaCl; [b] Casted from a commercial SPES powder.

4. Conclusion

In this work, a series of S-PES with various *DS* were successfully fabricated by sulfonation of PES precursor using chlorosulfonic acid. The S-PES membranes were prepared by casting through the solvent evaporation method. The correlation between the physical and electrochemical

properties of the fabricated S-PES membranes was investigated in detail with varying *DS*. There is a crucial interplay between various membrane properties that eventually drives the cation exchange performance. An increase in the number of introduced ionic groups (sulfonic acid groups) results in a more hydrophilic character, higher *WU*, higher *IEC*, and higher ionic conductivity. The produced S-PES membrane with an optimum *DS* of 32.4% has an outstanding ionic conductivity of 16.85 mS cm^{-1} and an almost ideal permselectivity of 98.0% (in 0.5 M NaCl). This membrane shows a significant improvement in the trade-off between ionic conductivity and permselectivity compared to previously reported S-PES membranes and commercial benchmark CEMs. Therefore, these fabricated S-PES membranes are promising CEMs, especially for ED and RED.

Supporting Information

The following file is available free of charge

Additional experimental data (DOC/PDF)

Sulfonation reaction kinetics; Photographs of the precipitated S-PES pellets; Calculated *DS* at different reaction times using different techniques; SEM images of S-PES membrane; FT-IR, ^{1}H-NMR, TGA, and DTA analysis for PES and S-PES. Stress-strain curves of wet PES and S-PES membranes; Area resistance and water uptake of the fabricated S-PES membranes as a function of reaction time and *DS*; Permselectivity of S-PES and previously reported CEMs as a function of water uptake.

AUTHOR INFORMATION

Corresponding Author

Izumi Ichinose

Research Center for Macromolecules and Biomaterials, National Institute for Materials Science, 1-1 Namiki, Tsukuba 305-0044, Japan.

E-mail: ICHINOSE.Izumi@nims.go.jp

CRediT authorship contribution statement

Hussien K. Srour: Writing – original draft, Visualization, Methodology, Investigation, Formal analysis, Data curation, Conceptualization. Mizuki Inoue: Writing – review & editing, Methodology, Investigation. Edhuan Ismail: Writing – review & editing, Methodology, Investigation. László Szabó: Writing – review & editing. Minato Higa: Conductivity and permselectivity measurements. Mitsuru Higa: Conductivity and permselectivity measurements, Conceptualization. Izumi Ichinose: Writing – review & editing, Supervision, Funding acquisition, Conceptualization.

Acknowledgment

Part of this work was supported by the Council for Science, Technology and Innovation (CSTI), Cross-ministerial Strategic Innovation Promotion Program (SIP), the 3rd period of SIP "Creating a materials innovation ecosystem for industrialization" Grant Number JPJ012307 (Funding agency: NIMS). The first author would also like to acknowledge Cairo University, Giza, Egypt, for the research and educational support.

References

(1) Hong, J. G.; Park, T. W.; Dhadake, Y. Property evaluation of custom-made ion exchange membranes for electrochemical performance in reverse electrodialysis application. *J. Electroanal. Chem.* **2019**, *850*, 113437. https://doi.org/10.1016/j.jelechem.2019.113437.

(2) Esposito, R.; Vincenzo, M. Di; Gopalsamy, K.; Ganesan, S.; Upadhyaya, L.; Grande, C.; Szekely, G.; Nunes, S. P. Membranes for the pervaporation of solvent azeotropes: From molecular to process design. *Chem. Eng. J.* **2025**, *515*, 163728. https://doi.org/10.1016/j.cej.2025.163728.

(3) Le, N. L.; Nunes, S. P. Materials and membrane technologies for water and energy sustainability. *Sustain. Mater. Technol.* **2016**, *7*, 1–28. https://doi.org/10.1016/j.susmat.2016.02.001.

(4) Hong, J. G.; Zhang, B; Glabman, S.; Uzal, N.; Dou, X.; Zhang, H.; Wei, X.; Chen, Y. Potential ion exchange membranes and system performance in reverse electrodialysis for power generation: A review. *J. Memb. Sci.* **2015**, *486*, 71–88. https://doi.org/10.1016/j.memsci.2015.02.039.

(5) Długołecki, P.; Nymeijer, K.; Metz, S.; Wessling, M. Current status of ion exchange membranes for power generation from salinity gradients. *J. Memb. Sci.* **2008**, *319*, 214–222. https://doi.org/10.1016/j.memsci.2008.03.037.

(6) Avci, A. H.; Rijnaarts, T.; Fontananova, E.; Profio, G. D.; Vankelecom, I. F.V.; De Vos, W. M.; Curcio, E. Sulfonated polyethersulfone based cation exchange membranes for reverse electrodialysis under high salinity gradients. *J. Memb. Sci.* **2020**, *595*.

https://doi.org/10.1016/j.memsci.2019.117585.

(7) Güler, E.; Elizen, R.; Vermaas, D. A.; Saakes, M.; Nijmeijer, K. Performance-determining membrane properties in reverse electrodialysis. *J. Memb. Sci.* **2013**, *446*, 266–276. https://doi.org/10.1016/j.memsci.2013.06.045.

(8) Klaysom, C.; Ladewig, B. P.; Lu, G. Q. M.; Wang, L. Preparation and characterization of sulfonated solyethersulfone for cation-exchange membranes. *J. Memb. Sci.* **2011**, *368*, 48–53. https://doi.org/10.1016/j.memsci.2010.11.006.

(9) Feng, S.; Sasaki, K.; Nishihara, M. Effect of sulfonation level on sulfonated aromatic poly(ether sulfone) membranes as polymer electrolyte for high-temperature polymer electrolyte membrane fuel cells. *Macromol. Chem. Phys.* **2016**, *217*, 2692–2699. https://doi.org/10.1002/macp.201600397.

(10) Zeng, G.; Yue, B.; Li, X.; Yan, L. Astonishing synergetic effect of proton conducting between phosphonic acid groups and triazolyl groups tethered simultaneously on poly(ether sulfone) backbone. *Solid State Ionics* **2018**, *320*, 100–112. https://doi.org/10.1016/j.ssi.2018.02.025.

(11) Zhang, X.; Yue, B.; Yan, L.; Zeng, G.; Tao, S. Improving the comprehensive performances of phosphonic acid functionalized poly(ether sulfone) by compositing with 1H-1,2,3-triazol-4-yl functionalized poly(ether sulfone). *Int. J. Hydrogen Energy* **2016**, *41*, 4740–4750. https://doi.org/10.1016/j.ijhydene.2016.01.076.

(12) Fang, L. F.; Kato, N.; Yang, H. Y.; Cheng, L.; Hasegawa, S.; Jeon, S.; Matsuyama, H. Evaluating the antifouling properties of poly(ether sulfone)/sulfonated poly(ether sulfone)

blend membranes in a full-size membrane module. *Ind. Eng. Chem. Res.* **2018**, *57* (12), 4430–4441. https://doi.org/10.1021/acs.iecr.8b00114.

(13) Unveren, E. E.; Erdogan, T.; Çelebi, S. S.; Inan, T. Y. Role of post-sulfonation of poly(ether ether sulfone) in proton conductivity and chemical stability of its proton exchange membranes for fuel cell. *Int. J. Hydrogen Energy* **2010**, *35*, 3736–3744. https://doi.org/10.1016/j.ijhydene.2010.01.041.

(14) Cassady, H. J.; Cimino, E. C.; Kumar, M.; Hickner, M. A. Specific ion effects on the permselectivity of sulfonated poly(ether sulfone) cation exchange membranes. *J. Memb. Sci.* **2016**, *508*, 146–152. https://doi.org/10.1016/j.memsci.2016.02.048.

(15) Rochow, M. F.; Cassady, H. J.; Hickner, M. A. Methodology for selecting anion and cation exchange membranes based on salt transport properties for bipolar membrane fabrication. *ACS Appl. Polym. Mater.* **2025**, *7* (9), 5456–5464. https://doi.org/10.1021/acsapm.5c00148.

(16) Komuta, K.; Kakihana, Y.; Higa, M. Evaluation of donnan dialysis using a cation exchange membrane made of sulfonated polyether sulfone. *Salt Seawater Sci. Technol.* **2022**, *2*, 37–38. https://doi.org/10.11457/ssst.2.0_37.

(17) Rezayani, M.; Sharif, F.; Netz, R. R.; Makki, H. Insight into the relationship between molecular morphology and water/ion diffusion in cation exchange membranes: Case of partially sulfonated polyether sulfone. *J. Memb. Sci.* **2022**, *654* (April), 120561. https://doi.org/10.1016/j.memsci.2022.120561.

(18) Igaya, K.; Sakata, W. Methods for producing sulfonated aromatic polymers. Patent No. JPWO2013094586A1, 2013.

(19) Nolte, R.; Ledjeff, K.; Bauer, M.; Mülhaupt, R. Partially sulfonated poly(arylene ether sulfone) - A versatile proton conducting membrane material for modern energy vonversion technologies. *J. Memb. Sci.* **1993**, *83*, 211–220. https://doi.org/10.1016/0376-7388(93)85268-2.

(20) Kim, J. D.; Ohira, A.; Nakao, H. Chemically crosslinked sulfonated polyphenylsulfone (CSPPSU) membranes for PEM fuel cells. *Membranes.* **2020**, *10*. https://doi.org/10.3390/membranes10020031.

(21) Fauzi, F. B.; Kim, J. D. Comprehensive studies on sulfonated octaphenyl polyhedral silsesquioxane (SPOSS) using sulfuric acid: Structural analysis and composite crosslinked SPPSU/SPOSS membranes. *J. Memb. Sci.* **2024**, *702*, 122756. https://doi.org/10.1016/j.memsci.2024.122756.

(22) Sata, T.; Jones, G. N.; Sata, T. Properties, Characterization and Microstructure of Ion Exchange Membranes. In *Ion Exchange Membranes: Preparation, Characterization, Modification and Application*; The royal society of chemistry: London, UK, 2004; pp 94–98. https://doi.org/10.1039/9781847551177.

(23) Kakihana, Y.; Hashim, N. A.; Mizuno, T.; Anno, M.; Higa, M. Ionic transport properties of cation-exchange membranes prepared from poly(vinyl alcohol-b-sodium styrene sulfonate). *Membranes.* **2021**, *11*. https://doi.org/10.3390/membranes11060452.

(24) Higa, M.; Mizuno, T.; Anno, M. Characterization of cation-exchange membranes prepared from PVA-based block copolymers. *Bull. Soc. Sea Water Sci. Japan* **2016**, *70*, 324–325.

(25) Moore, W. J. *Basic Physical Chemistry*; Prentice-Hall, Inc.: New Jersey, USA., 1983.

(26) Huang, R. Y. M.; Shao, P.; Burns, C. M.; Feng, X. Sulfonation of poly(ether ether ketone)(PEEK): Kinetic study and characterization. *J. Appl. Polym. Sci.* **2001**, *82*, 2651–2660. https://doi.org/10.1002/app.2118.

(27) Hu, Y.; Yan, L.; Yue, B. Sulfonation mechanism of polysulfone in concentrated sulfuric acid for proton exchange membrane fuel cell applications. *ACS Omega* **2020**, *5*, 13219–13223. https://doi.org/10.1021/acsomega.0c01252.

(28) Bishop, M. T.; Karasz, F. E.; Russo, P. S.; Langley, K. H. Solubility and properties of poly(aryl ether ketone) in strong acids. *Macromolecules* **1985**, *18*, 86–93. https://doi.org/10.1021/ma00143a014.

(29) Reyna-Valencia, A.; Kaliaguine, S.; Bousmina, M. Tensile mechanical properties of sulfonated poly(ether ether ketone) (SPEEK) and BPO4/SPEEK membranes. *J. Appl. Polym. Sci.* **2005**, *98*, 2380–2393. https://doi.org/10.1002/app.22417.

(30) Barragán, V. M.; Pérez-Haro, M. J. Correlations between water uptake and effective fixed charge concentration at high univalent electrolyte concentrations in sulfonated polymer cation-exchange membranes with different morphology. *Electrochim. Acta* **2011**, *56*, 8630–8637. https://doi.org/10.1016/J.ELECTACTA.2011.07.060.

(31) Banerjee, S.; Kar, K. K. Impact of degree of sulfonation on microstructure, thermal, thermomechanical and physicochemical properties of sulfonated poly ether ether ketone. *Polymer.* **2017**, *109*, 176–186. https://doi.org/10.1016/j.polymer.2016.12.030.

(32) Thieu, L. M.; Zhu, L.; Korovich, A. G.; Hickner, M. A.; Madsen, L. A. Multiscale tortuous diffusion in anion and cation exchange membranes. *Macromolecules* **2019**, *52* (1), 24–35.

https://doi.org/10.1021/acs.macromol.8b02206.

(33) Jones, L.; Pintauro, P. N.; Tang, H. Coion exclusion properties of polyphosphazene ion-exchange membranes. *J. Memb. Sci.* **1999**, *162*, 135–143. https://doi.org/10.1016/S0376-7388(99)00132-5.

(34) Elozeiri, A. A. E.; Lammertink, R. G. H.; Rijnaarts, H. H. M.; Dykstra, J. E. Water content of ion-exchange membranes: Measurement technique and influence on the ion mobility. *J. Memb. Sci.* **2024**, *698*, 122538. https://doi.org/10.1016/j.memsci.2024.122538.

(35) Lakshminarayanaiah, N. Transport phenomena in artificial membranes. *Chem. Rev.* **1965**, *65*, 491–565. https://doi.org/10.1021/cr60237a001.

(36) Crabtree, J. M.; Glueckauf, E. Structural analysis of ion semi-permeable membranes by vo-ion uptake and diffusion studies. *Trans. Faraday Soc.* **1963**. https://doi.org/10.1039/TF9635902639.

(37) Sugimoto, Y.; Ujike, R.; Higa, M.; Kakihana, Y.; Higa, M. Power generation performance of reverse electrodialysis (RED) using various ion exchange membranes and power output prediction for a large RED stack. *Membranes.* **2022**, *12*. https://doi.org/10.3390/membranes12111141.

(38) Di Virgilio, M.; Basso Peressut, A.; Arosio, V.; Arrigoni, A.; Latorrata, S.; Dotelli, G. Functional and environmental performances of novel electrolytic membranes for PEM fuel cells: A lab-scale case study. *Clean Technol.* **2023**, *5*, 74–93. https://doi.org/10.3390/cleantechnol5010005.

(39) Feng, M.; Qu, R.; Wei, Z.; Wang, L.; Sun, P.; Wang, Z. Characterization of the thermolysis

products of Nafion membrane: A potential source of perfluorinated compounds in the environment. *Sci. Rep.* **2015**, *5*, 1–8. https://doi.org/10.1038/srep09859.

(40) Rand, A. A.; Mabury, S. A. Is there a human health risk associated with indirect exposure to perfluoroalkyl carboxylates (PFCAs)?. *Toxicology.* **2017**, *375*, 28–36. https://doi.org/10.1016/J.TOX.2016.11.011.

(41) DeWitt, J.C. Toxicological Effects of Perfluoroalkyl and Polyfluoroalkyl Substances. *Springer International Publishing*. **2015**. https://doi.org/10.1007/978-3-319-15518-0.

(42) Rivaton, A.; Gardette, J. L. Photodegradation of polyethersulfone and polysulfone. *Polym. Degrad. Stab.* **1999**, *66* (3), 385–403. https://doi.org/10.1016/S0141-3910(99)00092-0.

(43) Zha, H.; Xia, J.; Wang, K.; Xu, L.; Chang, K.; Li, L. Foodborne and airborne polyethersulfone nanoplastics respectively induce liver andlLung injury in mice: Comparison with microplastics. *Environ. Int.* **2024**, *183*, 108350. https://doi.org/10.1016/j.envint.2023.108350.

(44) Avci, A. H.; Messana, D. A.; Santoro, S.; Tufa, R. A.; Curcio, E.; Di Profio, G.; Fontananova, E. Energy harvesting from brines by reverse electrodialysis using Nafion membranes. *Membranes.* **2020**, *10*, 1–16. https://doi.org/10.3390/membranes10080168.

(45) Abidin, M. N. Z.; Nasef, M. M.; Veerman, J. Towards the development of new generation of ion exchange membranes for reverse electrodialysis: A review. *Desalination* **2022**, *537*, 115854. https://doi.org/10.1016/J.DESAL.2022.115854.

(46) Mehdizadeh, S.; Kakihana, Y.; Abo, T.; Yuan, Q.; Higa, M. Power generation performance of a pilot-scale reverse electrodialysis using monovalent selective ion-exchange membranes.

Membranes. **2021**, *11*, 1–25. https://doi.org/10.3390/membranes11010027.

(47) Długołęcki, P.; Gambier, A.; Nijmeijer, K.; Wessling, M. Practical potential of reverse electrodialysis as process for sustainable energy generation. *Environ. Sci. Technol.* **2009**, *43*, 6888–6894. https://doi.org/10.1021/es9009635.

For Table of Contents Only